Kinetic studies of the polymerization of an epoxy resin modified with rhodamine B

Raquel Fernández [a], Borja Fernández d'Arlas [a], Patricia A. Oyanguren [b], Iñaki Mondragon [a,*]

[a] 'Materials + Technologies' Group, Dept. of Chemical & Environmental Engineering, Polytechnic School, Universidad País Vasco/Euskal Herriko Unibertsitatea, Pza Europa 1, 20018 Donostia-San Sebastián, Spain
[b] INTEMA Univ. Nac. de Mar del Plata-CONICET, JB Justo 4302 Mar del Plata, Argentina

ABSTRACT

Novel fluorescent materials were satisfactorily synthesized. With this aim, an epoxy resin based on diglycidyl ether of bisphenol A (DGEBA) was reacted with a laser dye, rhodamine B (RB), to achieve an epoxy-based prepolymer. Then, a diamine, m-xylylenediamine (MXDA), was used as hardener with the purpose of obtaining a crosslinked polymer. The curing conditions strongly influence the intended final properties and the optimization of the curing requires a reliable kinetic model. For that reason, this work presents the kinetic study of the polymerization of the epoxy resin by differential scanning calorimetry (DSC) in isothermal mode as well as by Fourier transform infrared spectroscopy (FTIR). DSC data were fitted using a Kamal autocatalytic equation. Conversion as a function of reaction time curves obtained by means of both techniques agreed well. In addition, the synthesized epoxy-based materials were characterized by proton nuclear magnetic resonance spectroscopy (^{1}H NMR) and their fluorescent properties were also analysed.

© 2009 Elsevier B.V. All rights reserved.

1. Introduction

The unique properties of organic laser dyes offer access to a variety of applications in spectroscopy, optics and lasers. Rhodamine B (RB) is an important laser dye with excellent photophysical properties, such as long wavelength absorption and emission, high fluorescence quantum yield, large extinction coefficient and high stability against light [1–3]. These properties make this molecule useful for a large variety of applications, such as biological stains, water tracing agents, electrochemical luminescence sensitizers, molecular probes, chromoionophores in optical chemical sensors, solar collectors and many others [4–6]. Furthermore, recently, rhodamine-based fluorescent chemosensors for metal cations have received increasing interest [7–10].

Generally, this laser dye has three molecular forms (Fig. 1) when immersed in various media [11–13]. In a polar solvent, such as ethanol, the carboxyl groups participate in a typical acid–base equilibrium $RBH^+ \leftrightarrow RB + H^+$. Compounds I ($RBH^+$) and II (RB) are strongly coloured and emissive molecules. However, the equilibrium compound of lactone-containing molecule (III) is colourless and exhibits no emission, because the conjugated π-electron system in the chromophore is interrupted. The increase of temperature facilitates the transformation from RBH^+

(I) and RB (II) to lactone-containing molecule (III) to some extent [14].

On the other hand, epoxy resins have found extensive use in many industrial applications. In most of these applications, the desired product properties are obtained following a cure process involving the reactions between the epoxy and a curing agent. Indeed, it is possible to tailor and improve these properties for specific applications, choosing between the wide variety of curing agents and epoxy resins available. In this context, the preparation of novel materials based on an epoxy resin could be interesting.

The incorporation of a laser dye into a polymer matrix attempts to combine the photophysical properties of the dye and the physical properties of polymers. In particular, thermosetting epoxy polymers distinguish due to their advantageous mechanical, thermal and electrical properties, as well as their excellent adherence to different kinds of materials. There are examples in the literature, like the one reported by Li et al. [15], which combined in a composite the luminescent properties of a europium complex and the mechanical properties of an epoxy matrix. It is important to select adequately material hosts which disperse well the dye molecules, and for which laser efficiency and operational photostability are high [16]. Moreover, it is also of great interest the development of novel temperature sensitive paints (TSP) containing RB. Conventional TSP consists of a luminescent dye embedded in a film of an oxygen permeable polymer. Several authors have reported the synthesis of different TSP, such as Obata et al., which developed a temperature sensing polymer film based on RB dye bearing

---

* Corresponding author.
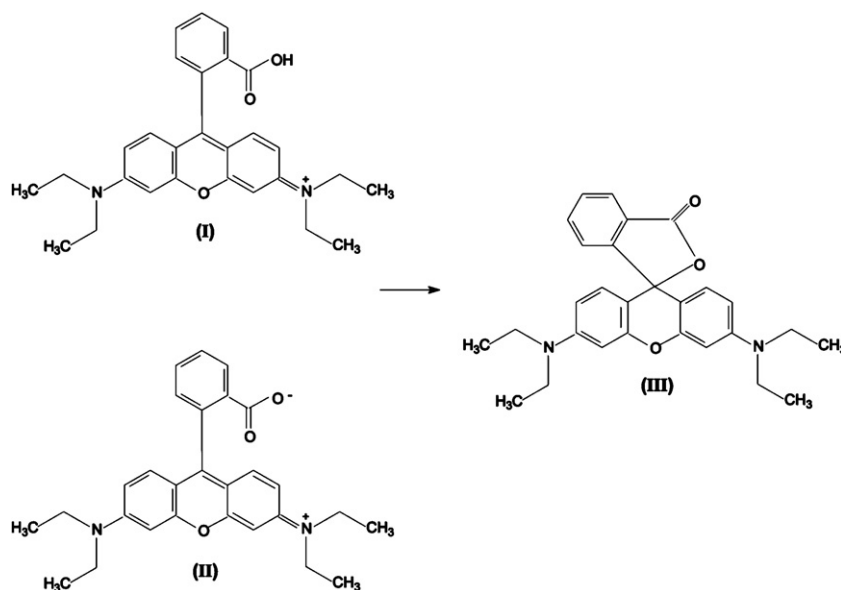E-mail address: inaki.mondragon@ehu.es (I. Mondragon).

Fig. 1. Molecular forms of rhodamine B.

poly(isobutyl methacrylate-*co*-2,2,2-trifluoroethyl methacrylate) [1]. With regards to this application, in the case of epoxy systems, they are very good candidates to be used as coatings, but the oxygen permeability of such matrices depends on the curing agent and the epoxy resin used [17].

Kinetic mechanisms of epoxy resin curing have been intensively studied in the past applying different models, methods and experimental techniques. Fourier transform infrared (FTIR) studies, in either middle (MIR) or near (NIR) regions, can generate both overall reaction kinetics and also the reaction rates of each single reaction through the monitoring of the intensity changes of the corresponding peaks of different functional groups. However, the complex nature of MIR spectra and the overlapping peaks make it a difficult technique to use in comparison with NIR spectroscopy. The NIR region encompasses bands that result from the harmonic overtones of fundamental and combination peaks associated with hydrogen atoms, which is why compounds containing O–H, N–H and/or C–H bonds are favourable to the analysis by NIR [18–25].

Kinetic models developed from kinetic analysis of differential scanning calorimetry (DSC) data have been also widely applied to the curing of epoxy resins [26–36]. With presumption that the heat flow as measured by DSC, dH/dt, is proportional to the rate of reaction, dx/dt, it is possible to determine the conversion at each time, x, directly from the experimental curve by partial integration:

$$x = \frac{1}{\Delta H_{\mathrm{T}}} \int_0^t \left(\frac{\mathrm{d}H}{\mathrm{d}t}\right) \mathrm{d}t \tag{1}$$

where ΔH_{T} stands for the total heat of reaction as determined by DSC scans.

Modelling of the curing process can be approached both mechanistically and phenomenologically. Mechanistic models consider the complete scheme of consecutive and competitive reactions which take place during curing, whereas phenomenological models are based on empirical or semi-empirical rate laws which explain the well-known autocatalytic behaviour of the epoxy/amine reaction.

The phenomenological kinetics of cure can be generally described as

$$\frac{\mathrm{d}x}{\mathrm{d}t} = k(T) f(x) \tag{2}$$

where dx/dt is the reaction rate, $k(T)$ is a constant depending only on temperature and $f(x)$ an unknown function of conversion.

$k(T)$ is usually represented by Arrhenius relationship:

$$k = A \exp\left(\frac{-E_{\mathrm{a}}}{RT}\right) \tag{3}$$

where E_{a} is the activation energy of the reaction, T the absolute temperature, R the universal gas constant, and A is the pre-exponential or frequency factor, which gives an idea of the association tendency of reacting molecules.

In Eq. (2), $f(x)$ is chosen according to experimental data and describes the reaction mechanism. There are many different proposed functions for $f(x)$. The simplest model corresponds to an nth-order kinetic expression:

$$f(x) = (1-x)^n \tag{4}$$

For an isothermal test, substitution of Eq. (4) into (2) yields Eq. (5) that predicts a maximum of the reaction rate at time = 0:

$$\frac{\mathrm{d}x}{\mathrm{d}t} = k(T)(1-x)^n \tag{5}$$

Then, if an isothermal process is characterized by a thermogram showing a maximum of the reaction rate at some point other than the reaction start, the kinetic model given by Eq. (5) cannot be applied and the so-called Kamal–Sourour autocatalytic model [34] must be used:

$$\frac{\mathrm{d}x}{\mathrm{d}t} = (k_1 + k_2 x^m)(1-x)^n \tag{6}$$

where the reaction orders (n, m) and kinetic constants (k_1, k_2) can be obtained using Kenny's iterative method [35] by means of DSC isothermal data.

Based on this knowledge, this contribution arose to generate novel materials based on an epoxy matrix modified with RB that exhibit fluorescence properties, and to study the curing kinetics of the epoxy resin by FTIR and DSC at several isothermal temperatures. Proton nuclear magnetic resonance spectroscopy (^{1}H NMR) was used to characterize reactants and reaction products, and fluorescence spectra of the synthesized materials were also analysed.

2. Experimental

2.1. Materials

A bifunctional epoxy resin, diglycidyl ether of bisphenol A (DGEBA, DER 332, $n = 0.03$), with an epoxy equivalent of 174 g equiv.$^{-1}$ was gently provided by Dow Chemical. Rhodamine B (RB) was purchased from Fluka and m-xylylenediamine (MXDA) was supplied by Aldrich.

2.2. Samples preparation

A laser dye (RB) with a melting temperature of 210–211 °C was chosen as fluorescent molecule. A thermoplastic prepolymer containing RB (TRB) was synthesized by reaction between RB and DGEBA. It was prepared in a stoichiometric ratio $r = $ RB equiv./DGEBA equiv. $= 0.2$, to achieve a reaction product with epoxy groups in the extreme of chains. The sample was prepared mixing DGEBA and the required amount of RB at 90 °C in an oil bath during 5 min, in order to obtain a homogeneous mixture. Then, reaction was carried out at 130 °C during 60 min.

The resulting TRB was blended with DGEBA and a diamine (MXDA) was used as hardener with the aim of developing a crosslinked polymer (TRB10/DGEBA/MXDA). TRB, MXDA and the amount of DGEBA necessary to have a stoichiometric ratio $r' = $ MXDA equiv./epoxy (TRB + DGEBA) equiv. $= 1$ were mixed at room temperature being TRB the 10 wt% of the whole of the reactive blend. In addition, a mixture of solvents (tetrahydrofuran:ethanol, 0.96:0.04) was added to homogenize the sample. After that, the solvents were removed by evaporation at room temperature. Polymerization was performed at 100 °C during 60 min.

2.3. Techniques

FTIR was performed using a Nicolet Nexus 670/870 Spectrometer. MIR spectra were taken using a potassium bromide (KBr) beam splitter, an infrared light source and a DTGS KBr detector. All spectra were obtained at 2 cm^{-1} resolution using 20 scans. Sandwiches of KBr were prepared as sample containers and were introduced in a temperature chamber from Specac. NIR data were obtained using a calcium fluoride beam splitter, a white light source and a MCT/A detector cooled with liquid nitrogen. All spectra were generated at 8 cm^{-1} resolution using 36 scans. A large core (600/630 μm) low O–H fused silica-type multimode optical fiber (3M's specialty optical fiber) was used. The fiber was characterized by an attenuation at 630 nm (15,000 cm^{-1}) of less than 50 dB/km, and a numerical aperture of 0.39 ± 0.02. Two fibers were used as received and transmitting legs SMA (SMART) connectors (supplied by Newark Electronics) were used to attach fiber legs to the fiber link. A short length (less than 10 mm) of the protective buffer was removed from the distal ends of fibers, which were then slipped into the capillary to the desired path length. The space between fiber ends was filled with the reactive mixture and the whole assembly was inserted into an oil bath at the required temperature.

High resolution ^{1}H NMR spectra of the reaction reactants and products were recorded using a Bruker 300 MHz spectrometer. Samples were dissolved to 10 wt% in deuterated dimethyl sulfoxide (DMSO). ^{1}H NMR chemical shifts were measured with respect to tetramethylsilane (TMS) as internal standard.

DSC measurements were carried out on a Mettler Toledo DSC 822 differential scanning calorimeter equipped with a sample robot TSO 801 RO. Nitrogen was used as purge gas (10 mL min^{-1}). Temperature and enthalpy were calibrated by using an indium standard. Curing was performed in sealed aluminum pans containing a sample weight of around 7 mg. Isothermal runs were performed at temperatures ranging from 95 to 115 °C.

Films were prepared by spin-coating onto clean glass slides using a P6700 spin-coater from Cookson Electronics. The spinner cycle program was as follows: 2000 rpm for 30 s, 4000 rpm for 10 s, and 8000 rpm for 20 s. In the case of TRB samples, spin-coated films were prepared from 5 wt% solutions in tetrahydrofuran:ethanol, 0.64:0.36. For TRB10/DGEBA/MXDA, spin-coated films were prepared from 5 wt% reactive mixture solutions in tetrahydrofuran:ethanol, 0.96:0.04. Then, reactive mixture films were cured in an oven at 100 °C.

Fluorescence spectroscopy data were recorded on a FELIX32 spectrophotometer from Photon Technology International (PTI). During the fluorescence measurements, the temperature effect on the fluorescence of both materials was determined by passing a thermostated fluid through the sample housing to maintain a defined temperature. The temperature range of the sample was changed from 0 to 80 °C by a digital temperature controller.

3. Results and discussion

Reactions taking place during the polymerization of RB and the epoxy resin were analysed. The evolution in MIR spectra of a RB/DGEBA mixture with $r = 0.2$, during reaction at 130 °C at various times is shown in Fig. 2a and b. As can be seen, the peak at 1755 cm^{-1}
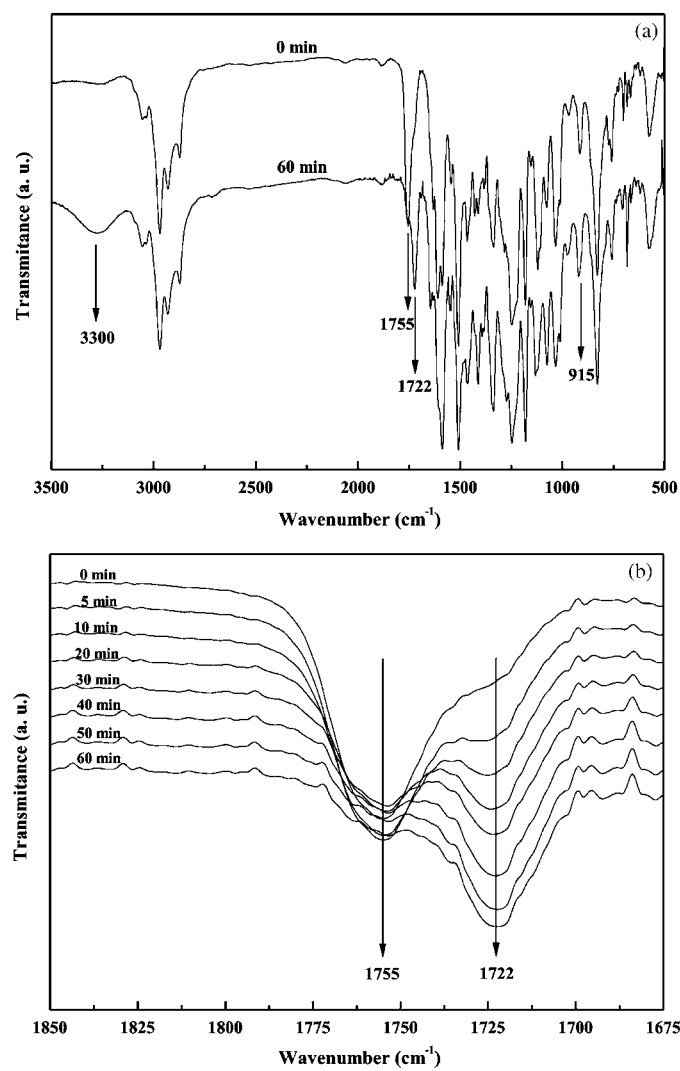

Fig. 2. MIR spectra of a RB/DGEBA mixture, $r = 0.2$, during reaction at 130 °C within the range: (a) 3500–500 cm^{-1} and (b) 1850–1675 cm^{-1}.

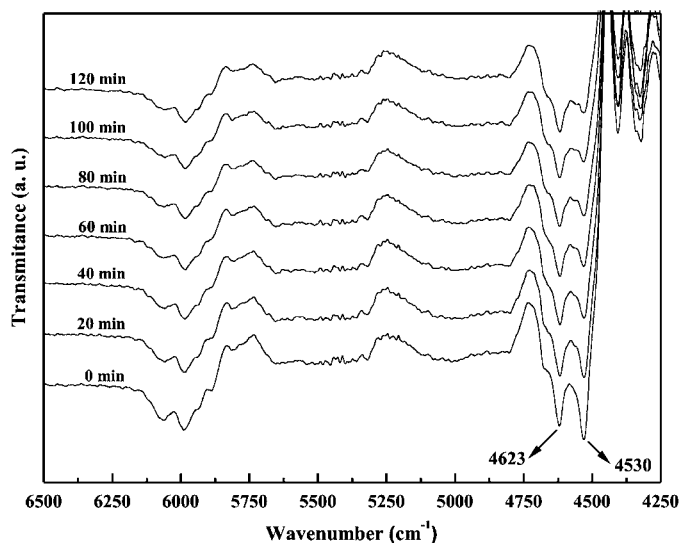**Fig. 3.** NIR spectra of a RB/DGEBA mixture, $r = 0.2$, during reaction at 130 °C.

arising from the stretching vibration of C=O of the carboxyl group of RB molecule diminished, while a new peak at 1722 cm^{-1}, which might correspond to the stretching vibration of C=O of an ester group, appeared. Furthermore, in Fig. 2a an increase of the peak corresponding to the stretching vibration of OH groups (3300 cm^{-1}) can be observed. Probably, these results are consequence of the condensation reaction between carboxyl groups of RB and epoxy groups of DGEBA. However, as the epoxy vibration peak at 915 cm^{-1} is overlapped with that corresponding to the asymmetric stretching vibration of C–O–C of RB at 920 cm^{-1} (Fig. 2a), in order to follow the evolution of epoxy groups during reaction, NIR data were collected. Fig. 3 shows a series of NIR spectra recorded at various reaction times during polymerization of RB/DGEBA, $r = 0.2$, at 130 °C. A progressive decrease in epoxy absorption (4530 cm^{-1}) during reaction can be observed in Fig. 3, confirming that condensation really took place.

Epoxy group conversion (X_{EP}) at any time t was calculated from the initial area of the peak at 4530 cm^{-1}, $A_{EP,0}$, with respect to the area of the reference peak at 4623 cm^{-1}, $A_{ref,0}$, and the corresponding values at time t, $A_{EP,t}$ and $A_{ref,t}$, according to the following equation:

$$X_{EP} = \frac{1 - (A_{EP,t})(A_{ref,0})}{(A_{EP,0})(A_{ref,t})} \tag{7}$$

Epoxy conversion vs. time curve obtained from NIR data is plotted in Fig. 4. As can be seen, the epoxy conversion after 60 min of reaction at 130 °C was around 0.2, which is the maximum theoretical value considering the stoichiometric ratio used ($r = 0.2$).

^{1}H NMR spectra were also taken for RB and DGEBA as well as for the reactive mixture, RB/DGEBA, $r = 0.2$, and the product of reaction at 130 °C during 60 min, TRB (Fig. 5a–c). In DGEBA spectra (Fig. 5a), H$_1$ protons correspond to those protons that are modified as a result of the condensation reaction between DGEBA and RB, whereas H$_6$ protons remain unchanged. Therefore, epoxy conversion (X'_{EP}) obtained from ^{1}H NMR data was calculated relating the areas of H$_1$ protons of RB/DGEBA, $r = 0.2$ ($A_{H1,RB/DGEBA}$) and TRB ($A_{H1,TRB}$), with respect to the areas of H$_6$ protons ($A_{H6,RB/DGEBA}$ and $A_{H6,TRB}$) in each case, according to the following equation:

$$X'_{EP} = \frac{(A_{H1,RB/DGEBA}/A_{H6,RB/DGEBA}) - (A_{H1,TRB}/A_{H6,TRB})}{A_{H1,RB/DGEBA}/A_{H6,RB/DGEBA}} \tag{8}$$

Applying Eq. (8), it was determined that X'_{EP} after 60 min of reaction at 130 °C was around 0.2, which is in agreement with the result

obtained by means of NIR. Besides, in Fig. 5c it is shown the appearance of new peaks between 4 and 6 ppm, which may correspond to new protons arising from RB/DGEBA, $r = 0.2$, reaction.

In consequence, 130 °C and 60 min were selected as reaction conditions with the aim of synthesizing a prepolymer (TRB) that subsequently could be dissolved in an epoxy/amine mixture. Therefore, the resulting TRB was blended with MXDA and the necessary amount of DGEBA to have a stoichiometric ratio r' = MXDA equiv./epoxy (TRB + DGEBA) equiv. = 1. Samples were prepared with 10 wt% of TRB, TRB10/DGEBA/MXDA (i.e., 0.036 wt% of RB).

Fig. 6 shows a set of NIR spectra recorded at various reaction times during TRB10/DGEBA/MXDA polymerization at 100 °C. Epoxy conversion vs. time curve was obtained in a similar manner than for TRB and it is shown hereinafter.

With regard to the kinetic analysis by means of DSC, Fig. 7 shows the isothermal DSC thermograms obtained at different curing temperatures. As temperature increases, the thermogram peak shifts toward shorter times being the whole process finished in less time.

To develop Kenny's iterative method [35], any reaction order was assumed. The main assumptions were that the cure mechanism is the same over all the temperature range studied and that $dx/dt = k_1$ when $x = 0$. Then, following this method, $n = 1.80$ and $m = 0.40$ values were determined for the range of temperatures studied. Isothermal DSC thermograms expressed in terms of reaction rate as a function of conversion are plotted in Fig. 8. As inferred from the figure, DSC experimental data fitted well to Eq. (6). The non-zero initial reaction rate characterized all the experiment curves, confirming an autocatalytic kinetic behaviour. According to these results, the global reaction rate of the system studied here is close to $m + n = 2$, as achieved by other authors [27,35,36] for different systems.

Fig. 9 shows the Arrhenius plot for the obtained constants (k_1, k_2) using this method. Assuming Arrhenius-type behaviour, E_a and A parameters for both processes described by Eq. (6) were calculated from the plot of $\ln k$ vs. $1/T$. A summary of the obtained kinetic parameters is shown in Table 1. As can be observed, k_2 is approximately seven times higher than k_1 for all the temperatures studied and $E_{a1} > E_{a2}$, which is characteristic for epoxy-ring opening catalyzed by hydroxyl groups generated by the reaction [36]. What's more, the activation energy values presented in this work are slightly lower than those reported in the literature for this kind of systems [30]. This could be due to the fact that the presence of tertiary amine in RB chemical structure might catalyze the epoxy
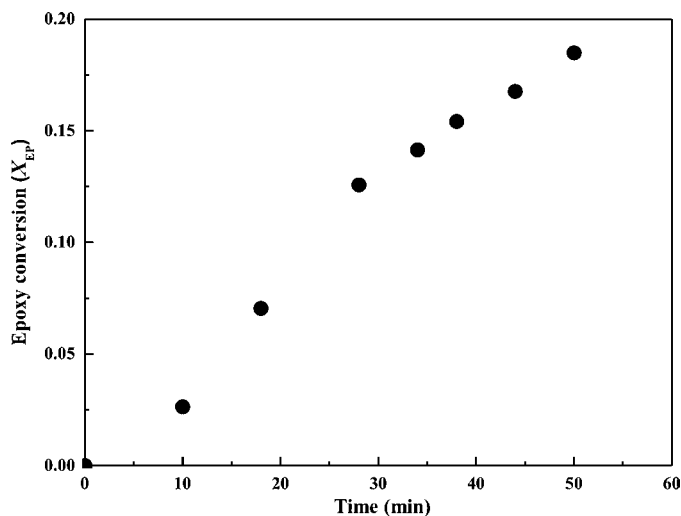

Fig. 4. Epoxy conversion (X_{EP}) as a function of time for a RB/DGEBA mixture, $r = 0.2$, during reaction at 130 °C.

group polymerization [37], contributing this way to a decrease in the activation energy values.

The developed model and the obtained parameters were used to predict the isothermal behaviour of the reacting system at the different temperatures used. With this aim, the model differential equations were integrated numerically to give time values at different conversions. Enough points were calculated in order to draw a neat curve. To draw each temperature isotherms by this method, the kinetic constants (k_1, k_2) obtained by Kenny's iteration [35] were used. The isothermal experimental curves and the obtained by this model, with $n = 1.80$ and $m = 0.40$, expressed in terms of conversion as a function of time are compared in Fig. 10. As can be seen, experimental data fitted well to the model predicted data for all the temperatures analysed, confirming the validity of the method used
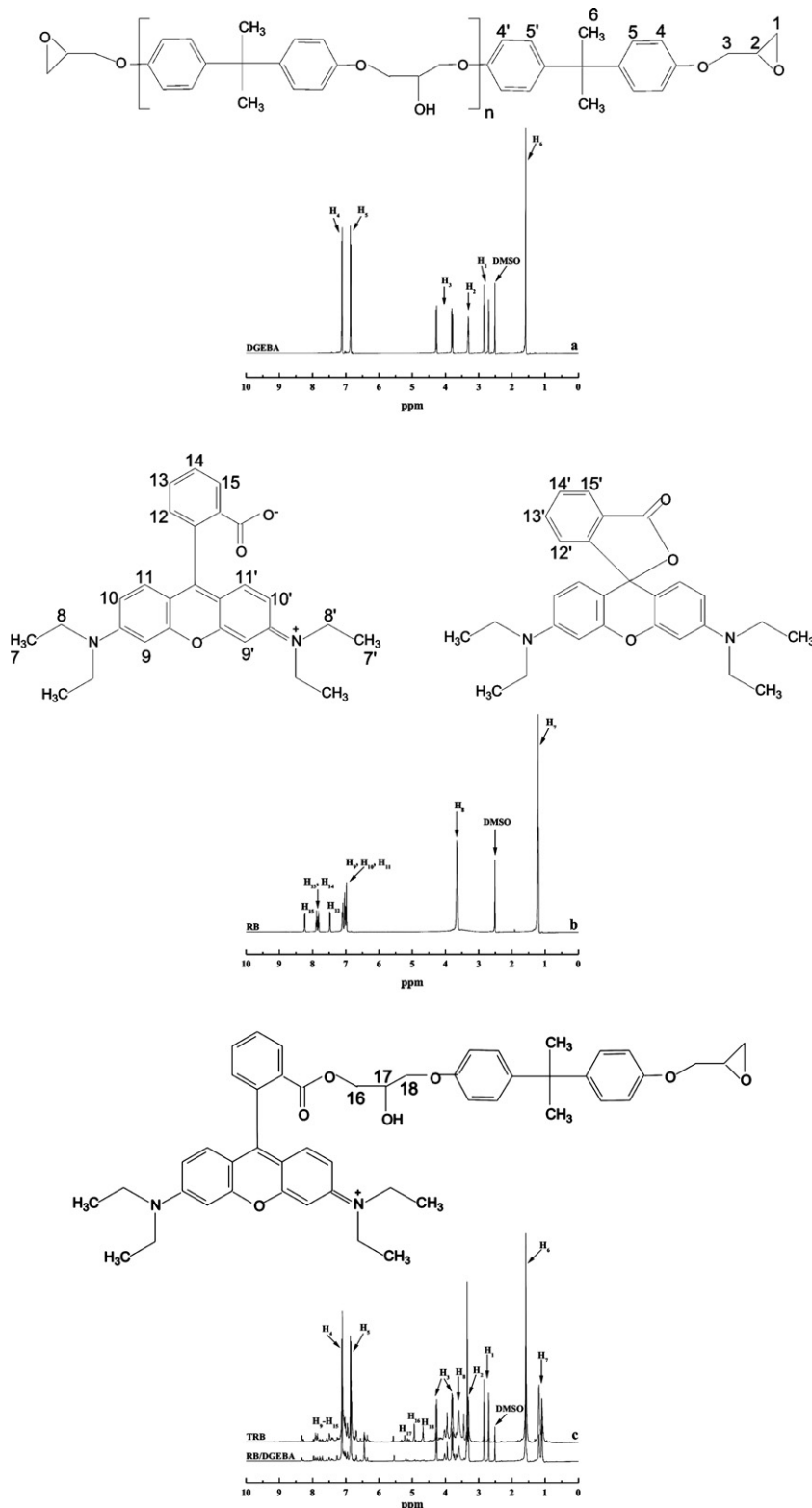
Fig. 5. ^{1}H NMR spectra of (a) DGEBA, (b) RB and (c) RB/DGEBA, $r = 0.2$, and TRB.

Table 1
General kinetic parameters of the autocatalytic model.

T (°C)	n	m	$k_1 \times 10^{-2}$ (min^{-1})	$k_2 \times 10^{-2}$ (min^{-1})	E_{a1} (kJ mol^{-1})	E_{a2} (kJ mol^{-1})	A_1 (min^{-1})	A_2 (min^{-1})
95			2.219	14.60				
100			2.739	17.24				
105	1.80	0.40	3.354	20.22	47.46	37.38	1.2×10^5	2.9×10^4
110			4.085	23.61				
115			4.957	27.50				
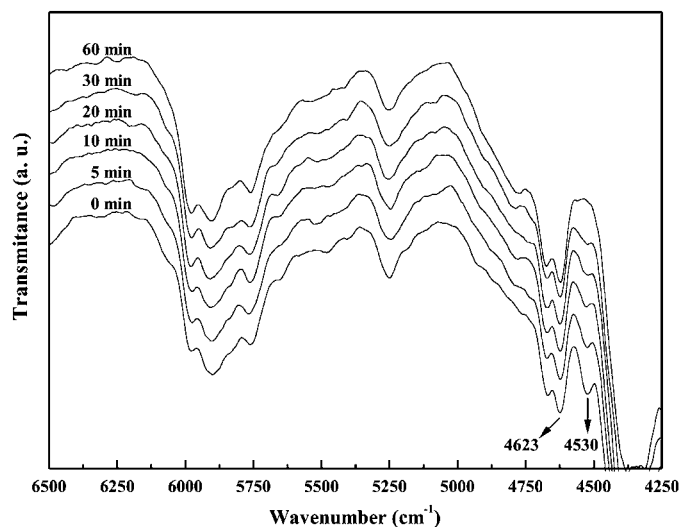
Fig. 6. NIR spectra of a TRB10/DGEBA/MXDA formulation during reaction at 100 °C.

Fig. 8. Comparison of experimental results (symbols) with the model obtained by iteration, with $n = 1.80$ and $m = 0.40$ (solid line), at different temperatures.

to determine the kinetic parameters and to represent the behaviour of the studied epoxy system.

Infrared conversion data obtained according to Eq. (7) for TRB10/DGEBA/MXDA polymerized at 100 °C, together with DSC conversion data obtained experimentally and by Kenny's method [35] at 100 °C are plotted in Fig. 11. As it is clear in the figure, good correlation was observed for both experimental techniques and the kinetic method used.

Finally, the fluorescence emission spectra for spin-coated films of the epoxy-based materials synthesized (TRB and TRB10/DGEBA/MXDA) are shown in Fig. 12. Also shown for comparison in the inner graph is the fluorescence emission spectrum of a 2×10^{-5} M solution of RB in ethanol. The spectra were taken using excitation wavelengths of 519, 530 and 564 nm for RB, TRB and
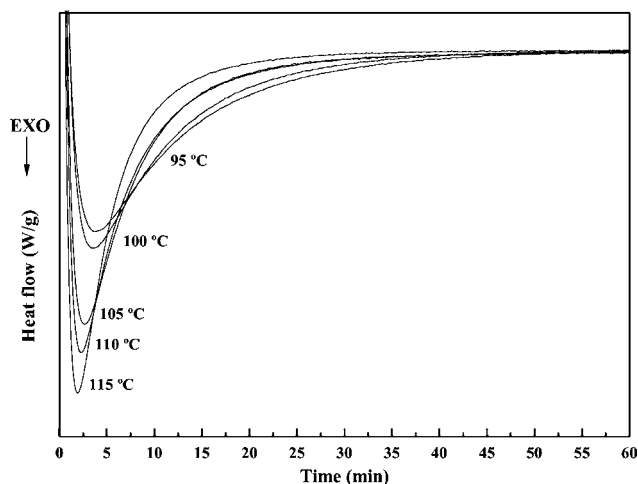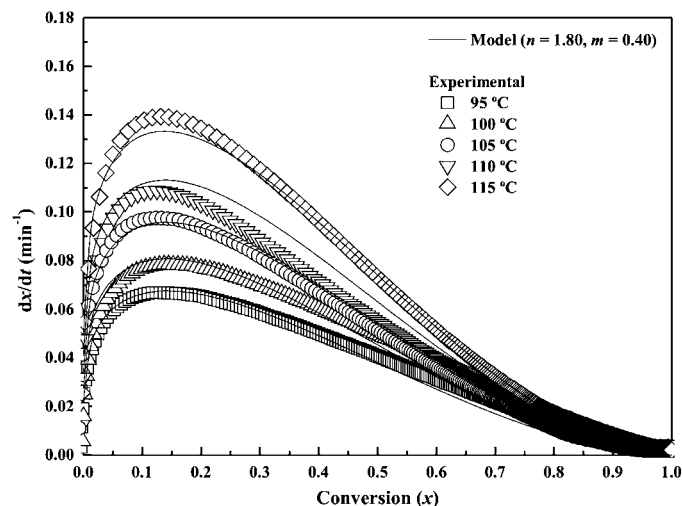
TRB10/DGEBA/MXDA, respectively. The maximum emission wavelength of RB was red shifted for TRB and TRB10/DGEBA/MXDA, probably as a result of the formation of new chemical bonds, though it also has to be taken into account that RB is in solution, and TRB and TRB10/DGEBA/MXDA in solid state [38]. Nonetheless, it is worth to note that after reactions the conjugated π-electron system in RB was not interrupted, leading to the satisfactory generation of epoxy-based polymers with fluorescent properties. Fig. 13 shows a plot of the normalized fluorescence intensities at maximum wavelength, for each one, of the spin-coated films of TRB and TRB10/DGEBA/MXDA as a function of temperature. The fluorescence intensity decreased linearly with increase of temperature, as it was also shown by other authors [1,14,38]. This temperature
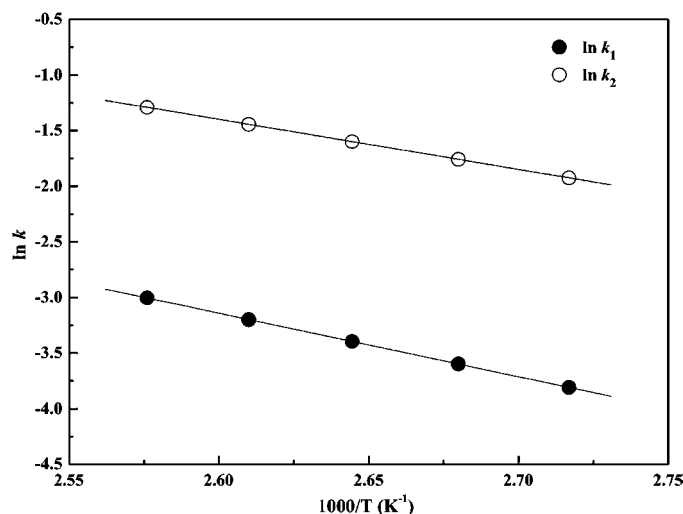

Fig. 7. DSC isothermal thermograms of TRB10/DGEBA/MXDA at different temperatures.

Fig. 9. Arrhenius plot for the Kamal model constants, calculated using Kenny's method.
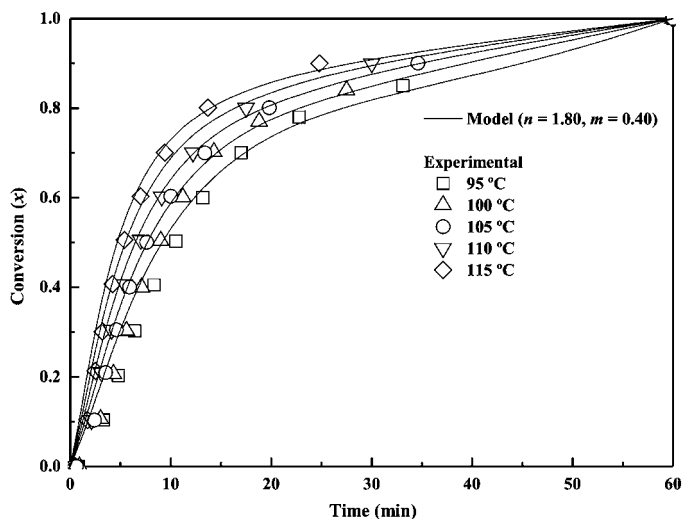
Fig. 10. Comparison between model predictions (solid line) and experimental results (symbols) obtained in isothermal DSC tests at different temperatures.
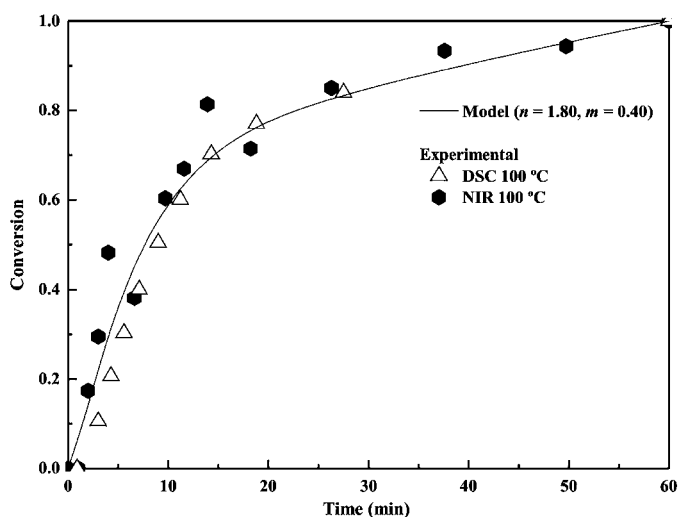

Fig. 11. Comparison between model predictions (solid line) and experimental results (symbols) obtained by DSC and NIR at 100 °C.
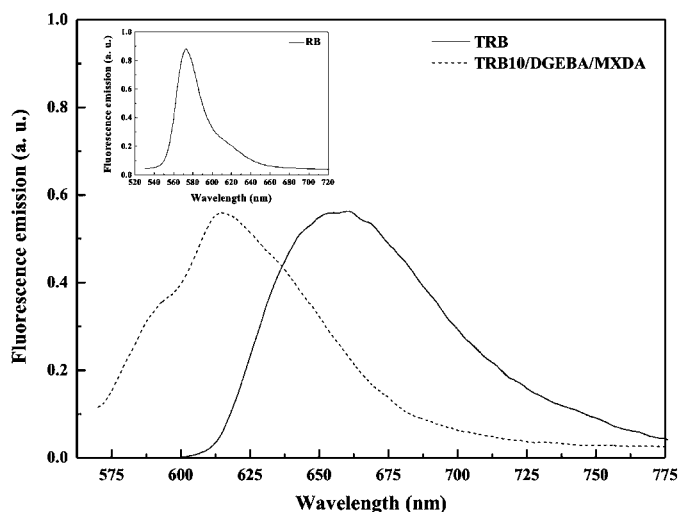

Fig. 12. Fluorescence emission spectra of TRB and TRB10/DGEBA/MXDA. The inset shows the fluorescence emission spectrum of RB.
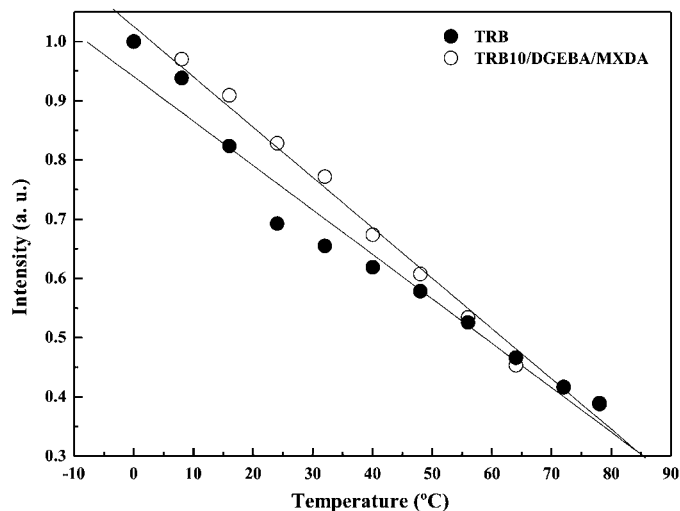

Fig. 13. Normalized luminescence intensity at maximum wavelength of TRB and TRB10/DGEBA/MXDA as a function of temperature.

sensitivity of the fluorescence can be advantageous for TRB and TRB10/DGEBA/MXDA to become multifunctional materials to probe temperature.

4. Conclusions

Curing kinetics of a novel epoxy-based system was studied by means of DSC, FTIR and ^{1}H NMR. Polycondensation of the epoxy resin and RB was verified by FTIR and ^{1}H NMR.

Cure kinetics of TRB10/DGEBA/MXDA formulation was successfully fitted to Kamal–Sourour generalized autocatalytic equation. The method selected to calculate the parameters of the autocatalytic-like kinetic model of cure was also used to predict the reaction conversion as a function of time at different temperatures. Furthermore, a good agreement between predictions of the model and experimental data was achieved.

Catalytic influence of hydroxyl groups formed by epoxy/amine addition on the reaction of cure was also determined. As the activation energy values obtained were slightly lower than those reported by other authors for similar systems, it can be concluded that the presence of tertiary amine from RB in the reaction media could catalyze the epoxy group polymerization.

Fluorescence emission spectra were also taken for TRB and TRB10/DGEBA/MXDA formulation, confirming that the conjugated π-electron system in RB was not interrupted as consequence of reactions. In addition, the dependence of the fluorescence intensity with temperature for both epoxy-based polymers was demonstrated, indicating that these materials could be used in applications in the area of fluorescent temperature sensors.

References

[1] M. Obata, M. Morita, K. Nakase, K. Mitsuo, K. Asai, S. Hirohara, S. Yano, J. Polym. Sci. A: Polym. Chem. 45 (2007) 2876.
[2] I. Zareba-Grodz, R. Pazik, K. Hermanowicz, W. Strek, K. Maruszewski, J. Lumin. 119–120 (2006) 148.

[3] N.O. Mchedlov-Petrossyan, N.A. Vodolazkaya, A.O. Doroshenko, J. Fluoresc. 13 (2003) 235.
[4] A. Silva, R.E.F. Boto, R.M. El-Shishtawy, P. Almeida, Eur. Polym. J. 42 (2006) 2270.
[5] T. Seçkin, A. Gültek, S. Kartaca, Dyes Pigments 56 (2003) 51.
[6] T. Ohishi, J. Non-Cryst. Solids 332 (2003) 80.
[7] Y. Xiang, Z. Li, X. Chen, A. Tong, Talanta 74 (2008) 1148.
[8] S. Bae, J. Tae, Tetrahedron Lett. 48 (2007) 5389.
[9] X. Zhang, Y. Shiraishi, T. Hirai, Tetrahedron Lett. 48 (2007) 5455.
[10] X.-F. Yang, X.-Q. Guo, H. Li, Talanta 61 (2003) 439.
[11] I. López Arbeloa, K.K. Rohatgi-Mukherjee, Chem. Phys. Lett. 128 (1986) 474.
[12] I. López Arbeloa, P. Ruiz Ojeda, Chem. Phys. Lett. 79 (1981) 347.
[13] I. Rosenthal, P. Peretz, K.A. Muszkat, J. Phys. Chem. 83 (1979) 350.
[14] F.-H. Ko, L.-Y. Weng, C.-J. Ko, T.-C. Chu, Microelectron. Eng. 83 (2006) 864.
[15] X.-F. Li, K.-T. Lau, Y. An, Y.-S. Yin, T. Wong, Mater. Lett. 62 (2008) 4434.
[16] T.H. Nhung, M. Canva, F. Chaput, H. Goudket, G. Roger, A. Brun, D.D. Manh, N.D. Hung, J.-P. Boilot, Opt. Commun. 232 (2004) 343.
[17] J. Lange, B. Nicolas, J. Galy, J.-F. Gerard, Polymer 43 (2002) 5985.
[18] R. Fernández, M. Blanco, M.J. Galante, P.A. Oyanguren, I. Mondragon, J. Appl. Polym. Sci. 112 (2009) 2999.
[19] L. Xu, J.H. Fu, J.R. Schlup, Ind. Eng. Chem. Res. 35 (1996) 963.
[20] L. Xu, J.R. Schlup, J. Appl. Polym. Sci. 67 (1998) 895.
[21] N.A. St. John, G.A. George, Polymer 33 (1992) 2679.
[22] G. Kortaberria, P. Arruti, N. Gabilondo, I. Mondragon, Eur. Polym. J. 40 (2004) 129.
[23] N. Salmon, V. Carlier, J. Schut, P.M. Remiro, I. Mondragon, Polym. Int. 54 (2005) 667.
[24] H. Liu, A. Uhlherr, R.J. Varley, M.K. Bannister, J. Polym. Sci. A: Polym. Chem. 42 (2004) 3143.
[25] J. Mijovic, S. Andjelic, J.M. Kenny, Polym. Adv. Technol. 7 (1995) 1.
[26] M. Blanco, M.A. Corcuera, C.C. Riccardi, I. Mondragon, Polymer 46 (2005) 7989.
[27] B. Fernández d'Arlas, L. Rueda, P.M. Stefani, K. De la Caba, I. Mondragon, A. Eceiza, Thermochim. Acta 459 (2007) 94.
[28] N. Sbirrazzuoli, S. Vyazovkin, Thermochim. Acta 388 (2002) 289.
[29] S. Vyazovkin, N. Sbirrazzuoli, Macromolecules 29 (1996) 1867.
[30] N. Sbirrazzuoli, S. Vyazovkin, A. Mititelu, C. Sladic, L. Vicent, Macromol. Chem. Phys. 204 (2003) 1815.
[31] K. Pielichowski, P. Czub, J. Pielichowski, Polymer 41 (2000) 4381.
[32] F. Chu, T. McKenna, S. Lu, Eur. Polym. J. 33 (1997) 837.
[33] R.B. Prime, Polym. Eng. Sci. 13 (1973) 365.
[34] M.R. Kamal, S. Sourour, Polym. Eng. Sci. 13 (1973) 59.
[35] J.M. Kenny, J. Appl. Polym. Sci. 51 (1994) 761.
[36] J. Macan, I. Brnardic, M. Ivankovic, H.J. Mencer, J. Therm. Anal. Calorim. 81 (2005) 369.
[37] B.A. Rozenberg, Adv. Polym. Sci. 75 (1985) 113.
[38] X. Guan, X. Liu, Z. Su, P. Liu, React. Funct. Polym. 66 (2006) 1227.